



# Development of IVIM for Perfusion Measurement in Thermal Therapies

Shalini Ranmuthu<sup>1</sup>, Samuel Fahrenholtz<sup>1,2</sup>, R. Jason Stafford<sup>1,2</sup>

<sup>1</sup> Department of Imaging Physics, UT MDACC; <sup>2</sup> UT Graduate School of Biomedical Sciences at Houston, UT Health

## Introduction

Magnetic resonance guided laser induced thermal therapy (MRgLITT) is a minimally invasive tumor ablation alternative to surgery.<sup>1</sup> Real-time MRI provides both soft-tissue contrast and quantitative temperature monitoring to guide LITT treatments. The presence of vasculature in the target tissue often results in unpredictable heating patterns due to convective losses associated with tissue perfusion, and has led to the development of biothermal models. However, these models require accurate, patient-specific parameter data, most of which is difficult to procure.<sup>2</sup> Here we investigate the potential of Intravoxel incoherent motion (IVIM)-MRI as a fast, reliable approach to quantify patient-specific perfusion parameters.

Perfusion is a measure of pseudo-random blood flow (microvasculature) normalized by tissue volume.<sup>3,4</sup> Both perfusion and diffusion are seen by IVIM, which then creates contrast between the two compartments by repeatedly imaging with magnetic diffusion gradients of increasing strength (higher 'b-values'). These gradients quickly dephase signal from the faster, more directional flow compartment and allow signal from more randomly diffusing media to remain (Figure 1).<sup>5</sup>

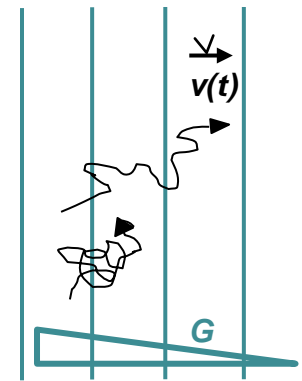


**Fig. 1:** Diagram of signal loss that occurs as particles move farther along the magnetic field gradients (G). Media with perfusion (top) traverses more of the gradient and loses more signal, but diffusion (bottom) loses less signal.<sup>5</sup>

## Theory

**Einstein's diffusion equation (Eq 1):**

$$\langle x^2 \rangle = D * q_i * t$$

where x is molecular displacement, D is diffusion coefficient, and  $q_i$  are the degrees of freedom.<sup>5</sup> We can solve for velocity (Eq 2):

$$v = \frac{\sqrt{\langle x^2 \rangle}}{t} = \sqrt{\frac{D * q_i}{t}}$$

**Mono-exponential model for IVIM (Eq 3)-** accurate for homogenous water compartments:

$$\frac{M}{M_0} = e^{(-b \cdot ADC)}$$

- $M_0$ : total reference signal intensity
- b: diffusion gradient factor
- ADC: apparent diffusion coefficient<sup>6</sup>

**Bi-exponential model for IVIM (Eq 4)-** accurate for media with multiple flow compartments:

$$M = M_0 \cdot [f_p \cdot e^{-b \cdot D^*} + (1 - f_p) \cdot e^{-b \cdot D}]$$

- $f_p$ : perfusion fraction
- $D^*$ : perfusing factor
- D: diffusing factor<sup>6</sup>

• MRI measures ADC, which can ideally be separated into D and  $D^*$

## Methods

**Phantom Construction** – A complex flow phantom was constructed to test IVIM measurements by filling a 2" wide x 8" long PVC pipe with a trimmed foam sponge. Water lines were attached to either side of the phantom using PVC caps adapted with connectors. The phantom was assembled and imaged underwater to eliminate trapped air bubbles (Figure 2). The water lines connected the phantom to a peristaltic pump and input/output reservoirs (Figure 3).

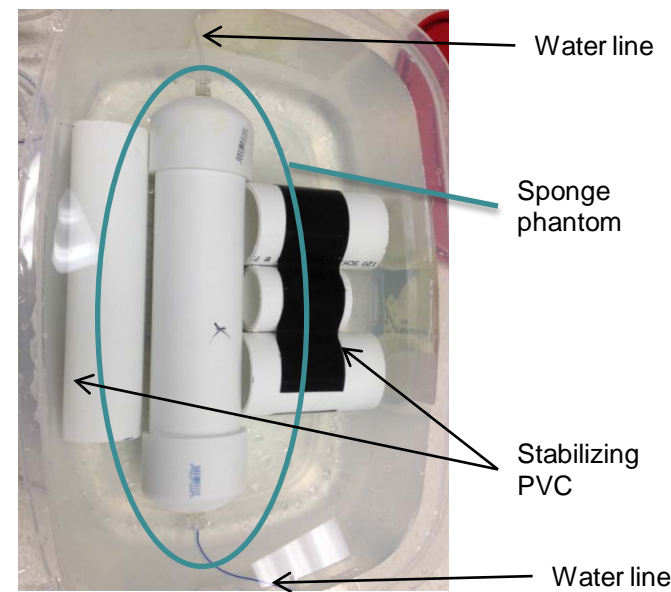


**Fig. 2:** Photo of submerged assembled phantom prepared for imaging with water lines attached and extra PVC sections to prevent motion while in MRI.

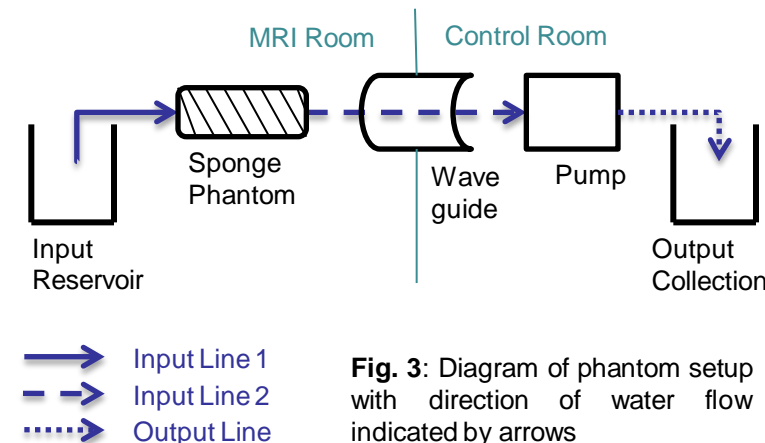


**Fig. 3:** Diagram of phantom setup with direction of water flow indicated by arrows

**MR Technique** – Images were acquired on a 3T clinical MRI scanner (Discovery MR750, GE Healthcare Technologies) using an 8 channel torso receiver array. Diffusion-weighted echo planar imaging (DW EPI) was employed with ASSET calibration (parallel-imaging approach). Diffusion gradients, characterized by 'b-value', were applied in all three orthogonal diffusion-sensitizing directions.

- 12 b-values: 25, 50, 75, 100, 125, 150, 200, 250, 350, 500, 750, 1000 sec/mm<sup>2</sup>
- TE / TR: Minimum (60.9 ms) / 6000 ms
- Freq FOV (R/L): 39 cm, Phase FOV (S/I): 0.7
- Freq 128 x Phase 128 matrix

**Data Analysis** – The mono and bi-exponential IVIM models (Eq 3, 4) were fit to the DW data within regions of interest (ROI) using a constrained nonlinear least squares algorithm in MATLAB. An additional MATLAB function was written to calculate flow velocity (Eq 1) from calculated IVIM data. Visualization of images was done with the Quantitative Utility for Assessing TreatmEnt RespOnse (QUATTRO) program.

## Results

Signal strength data from ROIs on the images were averaged across slices for each b-value. For images taken without flow in the phantom, a mono-exponential model was fit to the data (Eq 1). For images with phantom flow, the same process was used with the bi-exponential curve (Eq 2).

Free water with no phantom and no flow was imaged with different sequence repetition times (TR). TR of 2000 ms were too short to allow full  $T_1$  signal recovery (Figure 4), but a higher TR of 6000 ms demonstrated sufficient signal recovery.

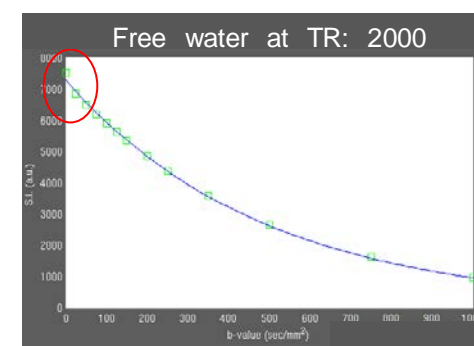


**Fig. 4:** Mono-exp model. The red circled area shows that the signal for b=0 was higher than expected, which suggests that TR is too short to allow magnetization to fully recover for other b-values.

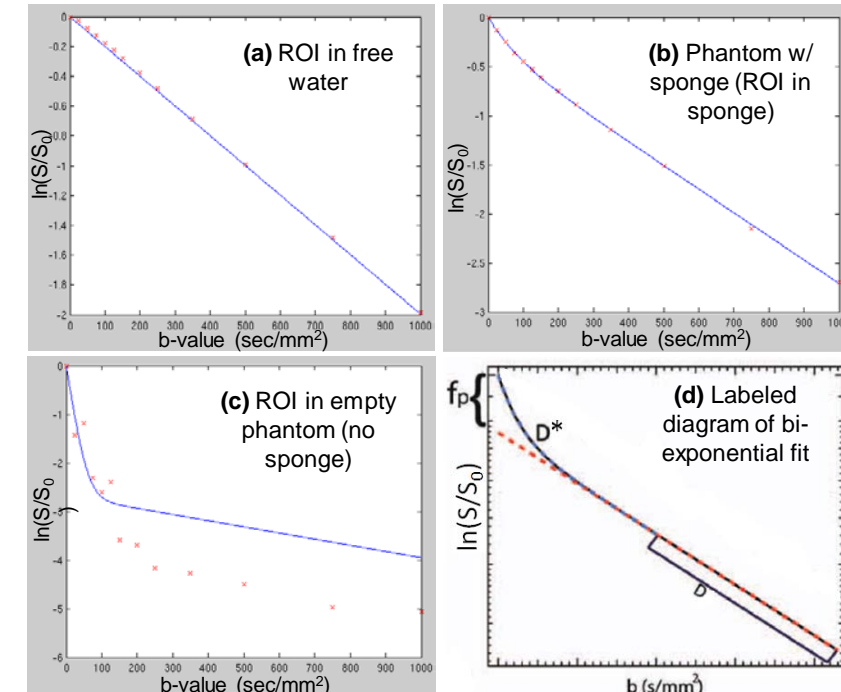


**Fig. 6:** Exponential fits of IVIM data (data= red, curve fit= blue). **a)** Looks mono-exponential, **b)** is more bi-exponential, **c)** may not be appropriate to fit to turbulent flow data, and **d)** demonstrates how IVIM parameters relate to exponential shape.<sup>6</sup>

**Table 1 (below):** IVIM data from fitting algorithm and velocity calculations from IVIM data. \*\*Measured velocity in blue was measured independent of MRI and was used to verify IVIM data and calculations.

| Image (ROI placement)             | ADC (mm <sup>2</sup> /sec) | D* (mm <sup>2</sup> /sec) | f <sub>p</sub> (%) | Velocity (mm/s) using ADC | Velocity (mm/s) using D* | Flow Present? |
|-----------------------------------|----------------------------|---------------------------|--------------------|---------------------------|--------------------------|---------------|
| Free water                        | 2.0E-03                    | 0                         | 0                  | 0.444                     | 0                        | N             |
| Phantom with sponge (sponge)      | 1.8E-03                    | 0                         | 0                  | 0.421                     | 0                        | N             |
| Empty phantom (left water)        | 1.3E-03                    | 47.9E-03                  | 93.16              | 0.358                     | 2.17                     | Y             |
| Empty phantom (right water)       | 2.2E-03                    | 6.7E-03                   | 9.92               | 0.466                     | 0.81                     | Y             |
| Phantom with sponge (sponge)      | 2.4E-03                    | 12.6E-03                  | 26.27              | 0.486                     | 1.11                     | Y             |
| Phantom with sponge (left water)  | 2.0E-03                    | 23.4E-03                  | 96.41              | 0.444                     | 1.52                     | Y             |
| Phantom with sponge (right water) | 2.3E-03                    | 0                         | 0                  | 0.476                     | 0                        | Y             |
| Measured velocity**               | n/a                        | n/a                       | n/a                | 0.4                       | 0.4                      | Y             |

When the phantom was connected to the pump, the measured flow rate was approximately 0.8 mL/sec. The velocity in the phantom was then calculated using the phantom geometry and continuity to be about 0.4 mm/s. All phantom images were taken with TR of 6000 ms and with water flowing from left to right of image.

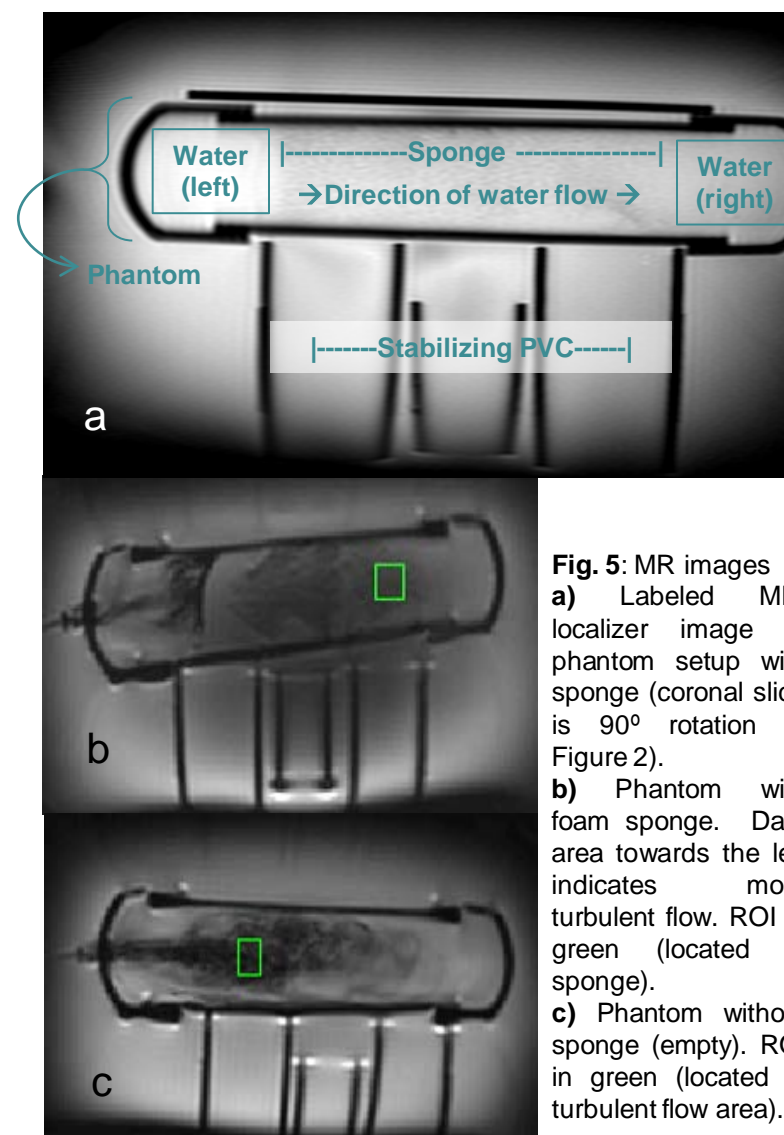


**Fig. 5:** MR images **a)** Labeled MRI localizer image of phantom setup with sponge (coronal slice is 90° rotation of Figure 2). **b)** Phantom with foam sponge. Dark area towards the left indicates more turbulent flow. ROI in green (located in sponge). **c)** Phantom without sponge (empty). ROI in green (located in turbulent flow area).

## Discussion

Perfusion is demonstrated by the presence of  $D^*$ ,  $f_p$ , and a bi-exponential fit, all of which are seen in the water flow through the sponge in the phantom (Figure 6b). Free water follows a mono-exponential curve (Figure 6a) with  $D^*$  and  $f$  values of 0, thus indicating a lack of compartmental flow (as expected). The water on the right hand side of the flowing sponge phantom has negligible  $D^*$  and  $f$ , similar to free water. This may be because IVIM cannot distinguish between laminar flow and diffusion (flow rate too slow), and phase contrast images could be taken to further investigate this effect. The water to the left of the sponge (unreasonably large  $f$ ) cannot be fit well by the bi-exponential model (Figure 6c). This suggests that IVIM is not appropriate for quantifying turbulent flow.

Velocity calculations using  $D^*$  were inaccurate, possibly due to inadequate perfusion. Velocities using ADC were close to the measured value regardless of actual flow presence, which may indicate that a faster flow rate is needed to differentiate from diffusion. A better flow rate to velocity calculation would also be necessary for accurate velocity comparisons.

## Acknowledgments / References

The authors would like to thank Ryan Bosca for providing source code and troubleshooting assistance for his QUATTRO program, and would also like to thank Florian Maier for his suggestions and feedback

1. Carpentier A, Itzcoovitz J, Payen D, et al. Real-time magnetic resonance-guided laser thermal therapy for focal metastatic brain tumors. *Neurosurgery* 2008;63:ONS21-9.
2. Fahrenholtz S, Stafford RJ, Maier F, et al. Generalised polynomial chaos-based uncertainty quantification for planning MRgLITT procedures. *Int J Hyperthermia* 2013;29:324-335.
3. Henkelman RM. Does IVIM measure classical perfusion?. *Magn Res Med* 1990;16:470-475.
4. Le Bihan D, Turner R. The capillary network: A link between IVIM and classical perfusion. *Magn Res Med* 1992;27:171-178.
5. Le Bihan D, Breton E, Lallemand D, et al. Separation of diffusion and perfusion in intravoxel incoherent motion MR imaging. *Radiology* 1988;168:497-505.
6. Cho GY, Sungheon K, Jensen JH, et al. A versatile flow phantom for intravoxel incoherent motion MRI. *Magn Res Med* 2012;67:1710-1720.